Journal of Experimental Botany, Vol. 64, No. 10, pp. 2943–2954, 2013
doi:10.1093/jxb/ert134 Advance Access publication 8 May, 2013
This paper is available online free of all access charges (see http://jxb.oxfordjournals.org/open_access.html for further details)

Journal of Experimental Botany
www.jxb.oxfordjournals.org

RESEARCH PAPER

Dynamic metabolic profiling of cyanobacterial glycogen biosynthesis under conditions of nitrate depletion

Tomohisa Hasunuma[1,2]*, Fumi Kikuyama[3], Mami Matsuda[1,2], Shimpei Aikawa[3], Yoshihiro Izumi[3] and Akihiko Kondo[3]

[1] Organization of Advanced Science and Technology, Kobe University, 1-1 Rokkodai, Nada, Kobe, 657–8501, Japan
[2] Precursory Research for Embryonic Science and Technology (PRESTO), Japan Science and Technology Agency, 3–5 Sanbancho, Chiyoda-ku, Tokyo 102-0075, Japan
[3] Department of Chemical Science and Engineering, Graduate School of Engineering, Kobe University, 1-1 Rokkodai, Nada, Kobe 657–8501, Japan

* To whom correspondence should be addressed. Email: hasunuma@port.kobe-u.ac.jp

Received 1 April 2013; Revised 1 April 2013; Accepted 18 April 2013

Abstract

Cyanobacteria represent a globally important biomass because they are responsible for a substantial proportion of primary production in the hydrosphere. *Arthrospira platensis* is a fast-growing halophilic cyanobacterium capable of accumulating glycogen and has the potential to serve as a feedstock in the fermentative production of third-generation biofuels. Accordingly, enhancing cyanobacterial glycogen production is a promising biofuel production strategy. However, the regulatory mechanism of glycogen metabolism in cyanobacteria is poorly understood. The aim of the present study was to determine the metabolic flux of glycogen biosynthesis using a dynamic metabolomic approach. Time-course profiling of widely targeted cyanobacterial metabolic intermediates demonstrated a global metabolic reprogramming that involves transient increases in the levels of some amino acids during the glycogen production phase induced by nitrate depletion. Also, *in vivo* labelling with $NaH^{13}CO_3$ enabled direct measurement of metabolic intermediate turnover in *A. platensis*, revealing that under conditions of nitrate depletion glycogen is biosynthesized with carbon derived from amino acids released from proteins via gluconeogenesis. This dynamic metabolic profiling approach provided conclusive evidence of temporal alterations in the metabolic profile in cyanobacterial cells.

Key words: ^{13}C, cyanobacteria, glycogen, *in vivo* labelling, metabolic turnover, metabolomics.

Introduction

Environmental concerns and the depletion of worldwide oil reserves have led many governments to promote research on environmentally benign and sustainable biofuels in order to enhance energy independence. Biofuel production from renewable biomass sources is one of the most promising alternatives to petroleum-based transport fuels. Biofuels are generally classified as either 'first-generation fuels' if they are produced from sugar/starch crops or 'second-generation fuels' if they are produced from lignocellulosic biomass feedstocks such as crop residues, grasses, sawdust, and wood chips (Mussatto et al., 2010; Hasunuma and Kondo, 2012). However, a major controversial issue related to biofuel production involves competition for arable land between producers of energy crops and producers of edible crops. The cultivation of terrestrial plants as energy resources is also limited by the availability of fresh water supplies (John et al., 2011; Quintana et al., 2011).

Photosynthetic algae are of considerable interest as an alternative renewable source of biomass for the sustainable

Abbreviations: 3PGA, 3-phosphoglycerate; ADP-Glc, ADP-glucose; CE/MS, capillary electrophoresis/mass spectrometry; ESI, electrospray ionization; F6P, fructose-6-phosphate; G1P, glucose-1-phosphate; G6P, glucose-6-phosphate; HPLC, high-performance liquid chromatography; LC/QqQ-MS, liquid chromatography/triple quadrupole mass spectrometry; PDA, photodiode array; Rubisco, ribulose-1,5-bisphoshate carboxylase/oxygenase; RuBP, ribulose-1,5-bisphoshate; TOF, time of flight.

production of biofuels. Biofuels produced from algal feedstocks are referred to as 'third-generation fuels' and their production does not compete directly with agriculture, as it requires neither productive land nor fresh water (Dismukes et al., 2008). Several species of algae can store significant amounts of energy-rich compounds such as lipids and polysaccharides (starch and glycogen) that can be utilized for the production of distinct biofuels, including biodiesel and bioethanol. Cyanobacteria are especially attractive because their photosynthetic and biomass production rates are higher than those of terrestrial plants (Dismukes et al., 2008; Quintana et al., 2011). In addition, as cyanobacteria are prokaryotes, their metabolic processes are more readily amenable to genetic modifications designed to enhance the production of energy-rich compounds than are those of eukaryotic algae. Cyanobacteria possess relatively small genomes, many of which have been sequenced. Thus, compared with eukaryotic algae, it is less complicated to utilize cyanobacteria in systems biology research (Rittmann, 2008; Weckwerth, 2011).

Glycogen, α-1,6-branched α-1,4-glucan, is the primary storage polysaccharide in cyanobacteria (Ball and Morell, 2003). Under conditions of optimal light intensity and nitrate supply, glycogen may accumulate to more than 50% of the dry weight of cyanobacterial cells (Aikawa et al., 2012). As glycogen can be converted into liquid biofuels such as ethanol, isobutanol, and butanol via fermentation process using microorganisms such as yeast and bacteria (John et al., 2011), enhancing the glycogen production capacity of cyanobacteria is a promising strategy for producing third-generation biofuels.

In cyanobacteria, glycogen is synthesized from CO_2 assimilated during periods of light exposure (Ball and Morell, 2003). Although nitrogen depletion and salt stress are known to impact glycogen accumulation in cyanobacteria (Page-Sharp et al., 1998; Yoo et al., 2007; Osanai et al., 2011), little is known about the mechanisms that regulate glycogen metabolism in these organisms. Understanding of the metabolic flux of glycogen biosynthesis in cyanobacteria is also quite limited.

Metabolic profiling has proven to be a powerful tool for gaining insights into functional biology (Garcia et al., 2008; Baran et al., 2009). The comprehensive analysis of a wide range of metabolites in cells using high-sensitivity mass spectrometry techniques makes it possible to identify metabolic compounds that play important roles in specific biological processes (Yoshida et al., 2008; Hasunuma et al., 2010, 2011).

So far, cyanobacterial metabolomics studies have mainly concentrated on the model cyanobacterial strain *Synechocystis* sp. PCC6830 (Eisenhut et al., 2008; Krall et al., 2009; Osanai et al., 2011). Eisenhut et al. (2008) performed metabolome phenotyping of inorganic carbon limitation in *Synechocystis* cells to analyse the metabolic process of low carbon acclimation. However, there has been no report demonstrating the temporal metabolic profile of *Synechocystis* cells cultivated under condition of nitrate deficiency. Recently, Aikawa et al. (2012) reported the usefulness of *Arthrospira platensis* as a glycogen supplier by comparing the glycogen capacity with α-polyglucan (glycogen and starch) production of other cyanobacteria and microalgae in the related studies. *A. platensis* is a filamentous non-N_2-fixing cyanobacterium that is potentially one of the algae capable of producing bioenergy and renewable energy because of their high growth ability in outdoor environments (Santillan, 1982), although the intracellular metabolite profile of *A. platensis* has never been characterized by the metabolomic approach.

In the present study, we quantified the level of primary metabolic intermediates such as sugar phosphates, sugar nucleotides, amino acids, and organic acids in *Synechocystis* sp. PCC6803 under conditions in which the glycogen level was increased by manipulating the nitrate supply. The metabolomics approach was applied to *A. platensis*. Metabolic turnover of these compounds was also assessed using an *in vivo* ^{13}C-labelling technique in order to directly measure the flow of carbon during glycogen biosynthesis. Our experiments revealed that glycogen produced during nitrate depletion is biosynthesized with carbon atoms derived from proteins rather than CO_2.

Materials and methods

Strains and culture conditions

A. platensis NIES-39, obtained from the Global Environmental Forum (Tsukuba, Japan), was grown in modified SOT liquid medium (Aikawa et al., 2012). *Synechocystis* sp. PCC6803 was grown in BG11 liquid medium (Rippka et al., 1979). Cultivations were carried out in 500 ml flasks containing 250 ml of SOT or BG11 medium; flasks were incubated in an NC350-HC plant chamber (Nippon Medical and Chemical Instruments, Osaka, Japan) under continuous irradiation with 50 µmol of white light photons m^{-2} s^{-1} (whole-day illumination) with 100 rpm agitation at 30 °C. Growth and cell density were determined by measuring the optical density at 750 nm (OD_{750}) using a Shimadzu UV mini spectrophotometer. Cell density was determined as the dry cell weight in the medium, as a linear correlation was observed between dry cell weight and optical density.

Analysis of cellular components (glycogen and protein)

Glycogen was extracted from cells as described previously (Ernst et al., 1984), with minor modifications. Cells (10 mg dry weight) in 200 µl of KOH (30%, w/v) were incubated in a heat block for 90 min at 95 °C and subsequently placed on ice. To precipitate glycogen, 600 µl of ethanol pre-chilled to 4 °C was added to each cell extract, which was then kept on ice for 1 h. The extracts were centrifuged at 3000*g* for 5 min at 4 °C. The resulting pellets were washed twice with cold ethanol and dried for 10 min at 60 °C in a heat block. Each dried sample was reconstituted in 100 µl of water and centrifuged at 10 000*g* for 5 min at 4 °C, and the supernatant was subjected to high-performance liquid chromatography (HPLC) analysis. The glycogen content was determined as described previously (Aikawa et al., 2012).

Protein was extracted as described previously (De Marsac and Houmard, 1988). Protein concentrations were determined using a Sigma QuantiPro BCA Assay Kit (Sigma-Aldrich, St Louis, MO, USA), with bovine serum albumin as the standard.

Spectral analysis

Cells cultivated for 3 d under the conditions described above were diluted with medium to adjust the OD_{750} to 0.3 for *A. platensis* and 0.1 for *Synechocystis*. Steady-state absorption spectra were collected

at room temperature as described previously (Akimoto et al., 2012) using a spectrometer equipped with an integrating sphere (JASCO V-650/ISV-722). Spectra were normalized to cell density (as estimated from turbidity at 750 nm), and the apparent OD_{750} was subtracted (Sarcina and Mullineaux, 2004).

Sampling procedure for metabolic profile analysis

Cell sampling was performed according to a previously reported method (Huege et al., 2011), with minor modifications. Cyanobacterial cells, equivalent to 5 or 10 mg dry weight, were removed from cultivation vessels and filtered using 10 µm (for *A. platensis*) or 1 µm (for *Synechocystis* sp. PCC6803) pore size Omnipore filter disks (Millipore, MA, USA). After washing with 260 mM (for *A. platensis*) or 20 mM (for *Synechocystis* sp. PCC6803) ammonium bicarbonate pre-chilled to 4 °C, cells retained on the filters were immediately placed into 2 ml of pre-cooled (–30 °C) methanol containing 190 nM (+)-10-camphorsulfonic acid, 31 µM L-methionine sulfone, and 31 µM piperazine-1,4-bis(2-ethanesulfonic acid) (PIPES) as internal standards for mass analysis. Intracellular metabolites were extracted using a cold 10:3:1 (v/v/v) methanol:chloroform:water solution, as described previously (Bölling and Fiehn, 2005). Cells were suspended by vortexing and then 1 ml of the cell suspension was mixed with 100 µl of pre-cooled (4 °C) water and 300 µl of chloroform containing 15 µM *trans*-β-apo-8'-carotenal as an internal standard for pigment analysis. The cell suspension was shaken at 1200 rpm (MBR-022UP; TAITEC, Saitama, Japan) for 30 min at 4 °C in the dark before centrifugation at 14 000*g* for 5 min at 4 °C. Next, 980 µl of cell extract obtained as the supernatant was transferred to a clean tube. After adding 440 µl of water, phase separation of aqueous and organic layers was performed by centrifugation at 14 000*g* for 5 min at 4 °C. Two aliquots (450 µl each) of the aqueous layer were transferred to clean tubes for analysis by capillary electrophoresis/mass spectrometry (CE/MS) and liquid chromatography/triple quadrupole mass spectrometry (LC/QqQ-MS). After filtration with a Millipore 5 kDa cut-off filter for the removal of solubilized proteins, the aqueous-layer extracts were evaporated under vacuum using a FreeZone 2.5 Plus freeze dry system (Labconco, Kansas City, MO, USA). Dried extracts were stored at –80 °C until used for mass analysis. A 50 µl aliquot of the organic layer obtained by phase separation was stored at –80 °C for subsequent pigment analysis.

CE/MS metabolite analysis

Dried metabolites were dissolved in 20 µl of Milli-Q water before CE/MS analysis. The CE/MS experiments were performed using an Agilent G7100 CE system, an Agilent G6224AA LC/MSD time-of-flight (TOF) system, and an Agilent 1200 series isocratic HPLC pump equipped with a 1:100 splitter for delivery of the sheath liquid. Agilent ChemStation software for CE and MassHunter software for the Agilent TOFMS were used for system control and data acquisition, respectively. The analytical conditions for cationic and anionic metabolite analyses were as described previously (Soga and Heiger, 2000; Hasunuma et al., 2011), with minor modifications as described below. The CE separations were performed in a fused silica capillary (1 m×50 µm i.d.) filled with 1 M formic acid (pH 1.8) as the electrolyte for cationic metabolite analyses or with 50 mM ammonium acetate (pH 9) for anionic metabolite analyses. The CE polarity was such that the electrolyte vial (inlet) was at the anode, and the electrospray ionization (ESI) probe (outlet) was at the cathode. Samples were injected into the CE system at a pressure of 50 mbar for 10 s for cation analyses or for 30 s for anion analyses. The voltage applied to the CE capillary was set at 30 kV, with a ramp time of 0.3 min. For anionic metabolite analyses, the electrolyte was passed through the capillary using an air pump, and was delivered at a pressure of 10 mbar from 0.4 to 30 min and 100 mbar from 30.1 to 49.5 min. The flow rate of the sheath liquid was set at 8 µl min^{-1}. The ESI-MS analyses were conducted in either the positive or negative ion mode using a capillary voltage of –3.5 or 3.5 kV, respectively. The TOF-MS fragmenter, skimmer, and Oct RFV were set to 100, 65, and 750 V, respectively. The flow of heated drying nitrogen gas (300 °C) was maintained at 10 l min^{-1}. Mass data were acquired at a rate of 1 spectra s^{-1} over the mass-to-charge ration (*m*/*z*) range 70–1000. The metabolites quantified using CE/MS are listed in Supplementary Table S1 at *JXB* online.

LC/QqQ-MS metabolite analysis

Dried extracts were dissolved in 50 µl of Milli-Q water and applied to an LC/QqQ-MS system (HPLC: Agilent 1200 series, MS: Agilent 6460 with Jet Stream Technology; Agilent Technologies) controlled with MassHunter Workstation Data Acquisition software v.B.04.01 (Agilent Technologies). The LC/QqQ-MS analyses were performed with multiple reaction monitoring (MRM), as described previously (Kato et al., 2012). The MRM parameters are listed in Supplementary Table S2 at *JXB* online.

Pigment analysis

Pigment extract (50 µl) was diluted to a final volume of 750 µl with a solution of 8:2 (v/v) acetonitrile:chloroform. Pigment content was analysed as described previously (Hasunuma et al., 2008) using an Acquity UPLC system (Waters, Milford, MA, USA). Pigment peaks were quantified using a photodiode array (PDA) detector set at a wavelength of 445 nm. The metabolites quantified using UPLC/PDA are listed in Supplementary Table S3 at *JXB* online.

^{13}C-labelling experiment

To analyse metabolic turnover in cyanobacteria, *in vivo* ^{13}C-labelling was performed using sodium ^{13}C-bicarbonate ($NaH^{13}CO_3$) as a carbon source. All cultures were grown at 30 °C at a photon flux density of 50 µmol m^{-2} s^{-1}. *A. platenis* cells (10 mg) pre-cultivated in SOT or nitrate-free SOT medium for 3 d were filtered and then resuspended to an initial OD_{750} of 1.0 in SOT or nitrate-free SOT medium containing 200 mM $NaH^{13}CO_3$. In addition, 5 mg of *Synechocystis* cells pre-cultivated in BG11 or nitrate-free BG11 medium for 3 d were filtered and then resuspended to an initial OD_{750} of 1.0 in BG11 or nitrate-free BG11 medium containing 25 mM $NaH^{13}CO_3$. After labelling for 1–30 min, 10 mg of *A. platenis* and 5 mg of *Synechocystis* cells were collected by filtration and processed as described in a previous section. Extracted intracellular metabolites were then analysed using CE/MS and LC/QqQ-MS. Mass spectral peaks of biological origin were identified manually by searching for mass shifts between ^{12}C- and ^{13}C-mass spectra. The ^{13}C fraction of metabolites and metabolic turnover rate were determined as described previously (Hasunuma et al., 2011).

Results

Glycogen production under conditions of nitrate depletion

Fig. 1A shows the glycogen and protein content of *A. platensis* cells grown under conditions of nitrogen depletion. *A. platensis* cells pre-cultivated under 50 µmol photons m^{-2} s^{-1} for 7 d at 30 °C in SOT medium containing 29.4 mM sodium nitrate as the nitrogen source were transferred to SOT medium and nitrate-free SOT medium at an initial OD_{750} of 0.6, corresponding to 0.53 g dry cells l^{-1}. Cells were then cultivated under continuous irradiation at 50 µmol photons m^{-2} s^{-1} at 30 °C. In the presence of nitrate, the glycogen and protein contents remained nearly constant. In contrast, in the absence of nitrate, the glycogen content increased to 63.2%

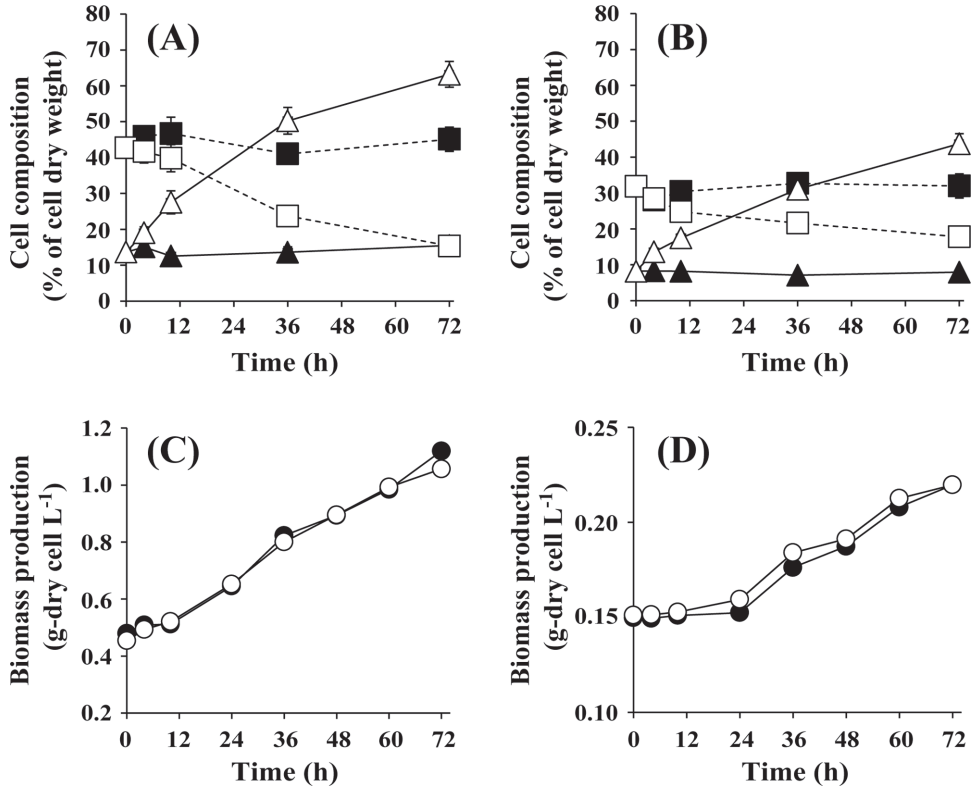

Fig. 1. Time-course analysis of the glycogen (triangles) and protein (squares) content of *A. platensis* (A) and *Synechocystis* sp. PCC6803 (B) cells, and concentration of *A. platensis* (C) and *Synechocystis* sp. PCC6803 (D) biomass during cultivation in the presence (closed symbols) and absence (open symbols) of nitrate.

of the dry cell weight while the protein content decreased to 15.4%. The density of cells in the presence and absence of nitrate was the same over the course of the 72 h cultivation (Fig. 1C). The same trends were observed for *Synechocystis* sp. PCC6803 cultured in the presence and absence of nitrate (Fig. 1B, D). Both the glycogen and protein content remained constant in cells cultivated in BG11 medium containing 17.6 mM sodium nitrate. Following transfer of cells to BG11 medium containing no nitrate, the glycogen content increased to 43.7% of the dry cell weight after 72 h.

Fig. 2 shows absorption spectra for *A. platensis* and *Synochocystis* cells grown under 50 µmol white light photons m^{-2} s^{-1}. In the normalized spectrum, four peaks are found, which are assigned to the chlorophyll Soret (~435 nm), carotenoid (~500 nm), phycobilisome (~620 nm), and chlorophyll Qy (0,0) (~676 nm) bands (Akimoto et al., 2012). In our experiments, nitrate depletion resulted in a decrease in the absorbance at 620 nm in both *A. platensis* and *Synechocystis* cells, indicating a decrease in the phycobilisome content. As the absorbance at 430 nm should indicate intracellular content of

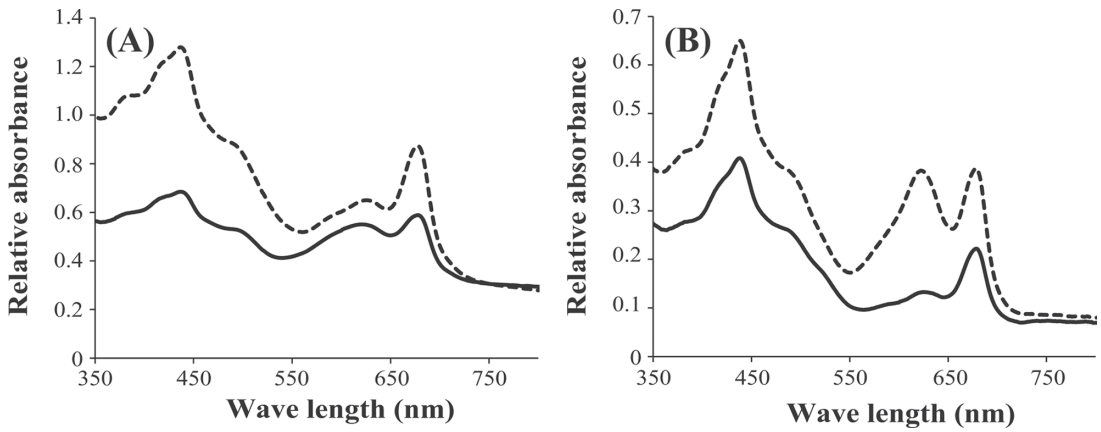

Fig. 2. Absorption spectra of *A. platensis* (A) and *Synechocystis* sp. PCC6803 (B) cells grown in SOT and BG11 medium, respectively, with (dashed line) or without (solid line) addition of sodium nitrate.

both chlorophyll *a* and carotenoids (Fraser et al., 2000), the decrease in the absorbance at 430 nm indicated a decrease in these pigments. Based on the pigment analysis, chlorophyll *a* and total carotenoid calculated as a sum of each carotenoid increased by the depletion of nitrate (Supplementary Tables S4 and S5 at *JXB* online).

Metabolic profile analysis of A. platensis *and* Synechocystis *sp. PCC6803*

Intracellular metabolites were extracted and identified in order to determine the metabolic profile of cyanobacteria during glycogen accumulation. Hydrophilic compounds, including amino acids, co-factors, nucleotides, organic acids, polyamines, sugar nucleotides, and sugar phosphates, were determined by CE/MS. Pigments were quantified by UPLC/PDA. The metabolites identified and quantified using CE/MS and UPLC/PDA are listed in Supplementary Tables S1 and S3. In *A. platensis*, 69 and five metabolites were detected by CE/MS and UPLC/PDA, respectively. In *Synechocystis* sp. PCC6803, 76 hydrophilic compounds and seven pigments were detected. The accumulation of metabolites in *A. platensis* and *Synechocystis* cells during 72 h of cultivation in the presence and absence of nitrate is summarized in Supplementary Tables S4 and S5.

The metabolite profiles of *A. platensis* and *Synechocystis* sp. PCC6803 cultivated for 72 h in the presence and absence of nitrate were compared using scatter plots (Fig. 3). In the presence of nitrate, the Spearman's rank correlation coefficient, r_s, was 0.6953. According to general statistical theory, an r_s of 0.60–0.79 is indicative of a strong correlation between the groups compared. In the absence of nitrate, we found a strong correlation between the metabolite profile of *A. platensis* and that of *Synechocystis* sp. PCC6803 (r_s=0.6680). These results indicated that nitrate depletion causes a similar perturbation in the metabolite profile of both species.

Temporal changes in metabolic profile under conditions of nitrate depletion

Changes in metabolite concentration in *A. platensis* cells over time are shown in Fig. 4. Glycogen is biosynthesized from the Calvin cycle intermediate fructose-6-phosphate (F6P) via glucose-6-phosphate (G6P), glucose-1-phosphate (G1P), and ADP-glucose (ADP-Glc) (Ball and Morell, 2003). No significant difference was observed with respect to the intracellular content of G1P and G6P in cells cultured in the presence and absence of nitrate (Fig. 4A). Nitrate-derived nitrogen is incorporated into glutamate in the form of ammonia by the enzyme glutaminase (Fig. 4B) (Flores et al., 2005). In the absence of nitrate, we found that the levels of some amino acids, such as alanine, asparagine, aspartate, glutamate, glutamine, and valine, decreased with time. In contrast, with the exception of glutamine, the levels of almost all other amino acids remained constant in nitrate-containing SOT medium. Notably, in *A. platensis* cells cultivated under conditions of nitrate depletion, there was a transient increase (until 12 h) in the levels of a number of amino acids, including glycine, histidine, isoleucine, leucine, methionine, phenylalanine, proline, threonine, and tyrosine. A transient increase in amino acid levels was also observed in *Synechocystis* sp. PCC6803 cells cultivated under conditions of nitrate depletion (Supplementary Fig. S1 at *JXB* online). These results raise the possibility that, when nitrate is missing, amino acids released from proteins are immediately assimilated into other metabolites, including sugar phosphates and glycogen.

Metabolite turnover under conditions of nitrate depletion

When metabolism is in a dynamic steady state *in vivo*, metabolites are replaced with newly synthesized compounds at a constant rate and the total amount of each metabolite remains unchanged. Thus, in order to fully understand metabolic flux

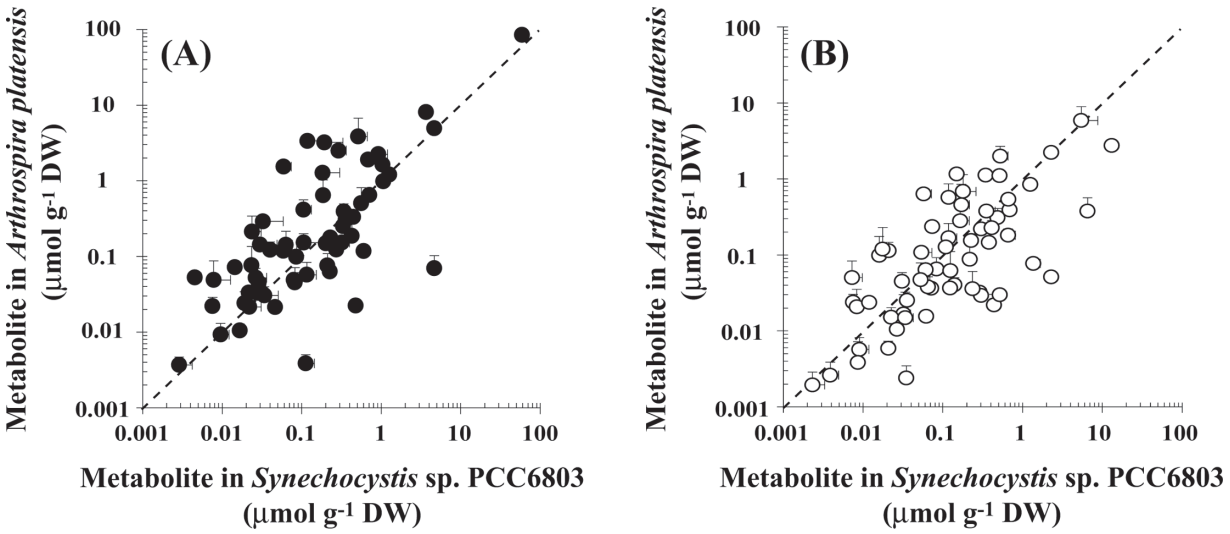

Fig. 3. Comparison of the metabolite content of *A. platensis* and *Synechocystis* sp. PCC6803 cells grown with (A) or without (B) the addition of sodium nitrate.

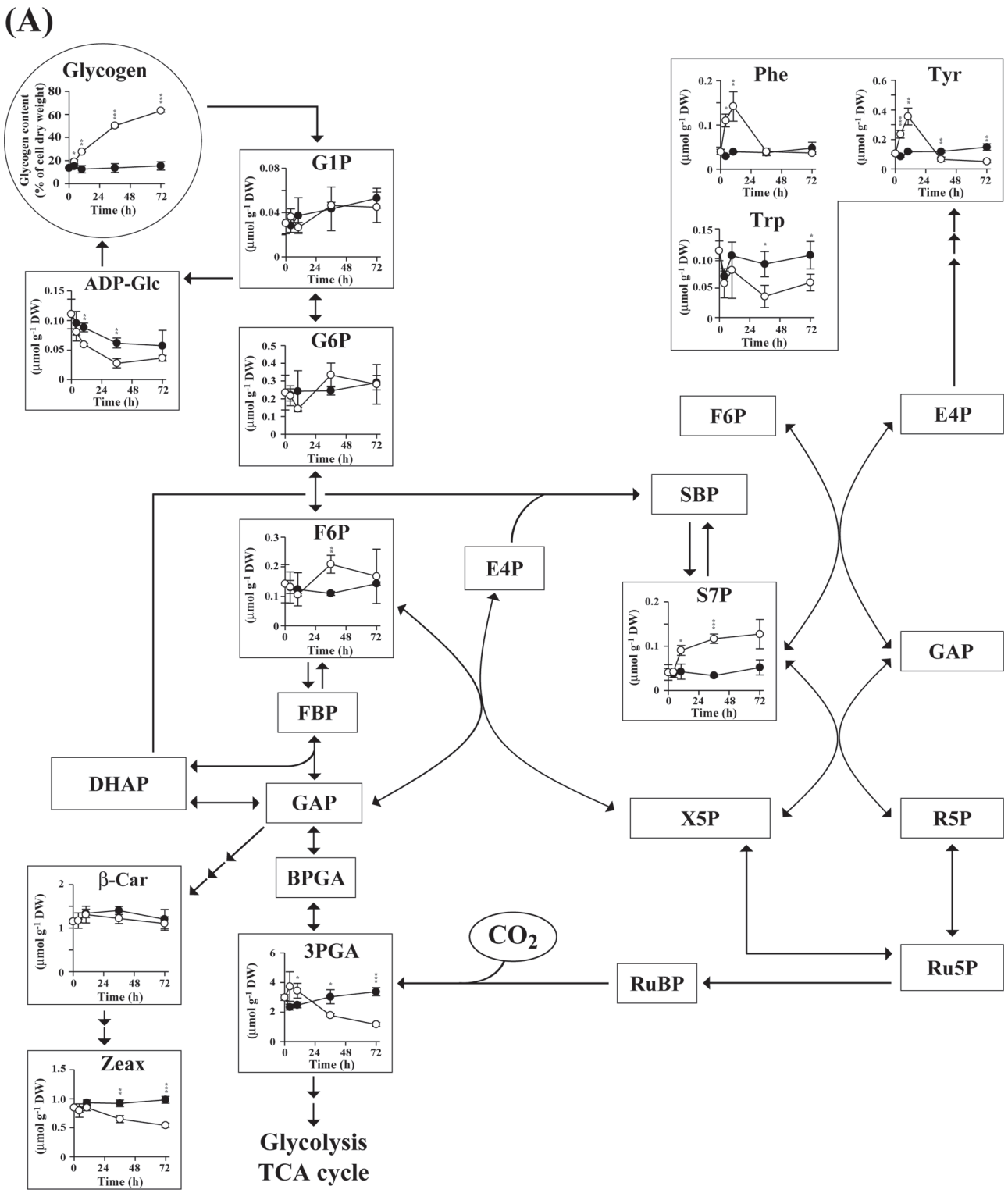

Fig. 4. Time-course analysis of the metabolite content of *A. platensis* cells cultivated with (closed circles) or without (open circles) the addition of nitrate. Error bars indicate ±standard deviation (SD) (n=3). Statistical significance was determined using Student's or Welch's t-test ($^{*}P$ <0.05, $^{**}P$ <0.01, $^{***}P$ <0.001). Abbreviations: AceCoA, acetyl-CoA; ADP-Glc, ADP-glucose; BPGA, 1,3-bisphosphoglycerate; β-Car, β-carotene; Carbamoyl-P, carbamoyl phosphate; Chl *a*, chlorophyll *a*; Cit, citrate; DHAP, dihydroxyacetone phosphate; E4P, erythrose-4-phosphate; FBP, fructose-1,6-bisphosphate; F6P, fructose-6-phosphate; Fum, fumarate; GAP, glyceraldehyde-3-phosphate; G1P, glucose-1-phosphate; G6P, glucose-6-phosphate; Icit, isocitrate; 2KG, 2-ketoglutarate; Mal, malate; OAA, oxaloacetate; PEP, phosphoenolpyruvate; 2PGA, 2-phosphoglycerate; 3PGA, 3-phosphoglycerate; Pyr, pyruvate; R5P, ribose-5-phosphate; Ru5P, ribulose-5-phosphate; RuBP, ribulose-1,5-bisphosphate; S7P, sedoheptulose-7-phosphate; SBP, sedoheptulose-1,7-bisphosphate; Suc, succinate; X5P, xylulose-5-phosphate; Zeax, zeaxanthin.

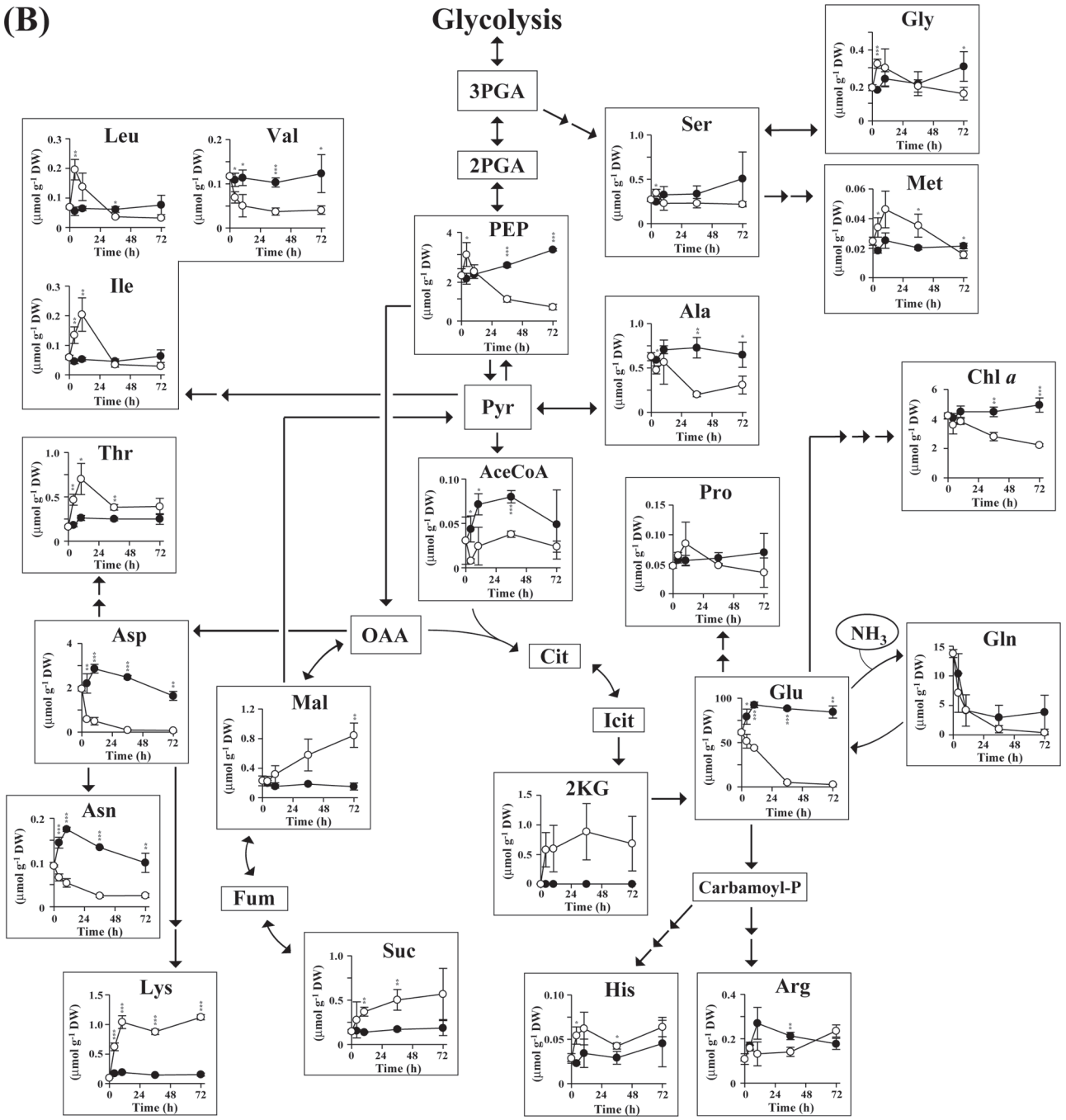

Fig. 4. *Continued*

related to glycogen biosynthesis, turnover of metabolic intermediates should be examined directly. In the present study, metabolic turnover, defined as the change in the ratio of carbon newly incorporated into metabolites to total metabolite carbon, was determined in the presence and absence of nitrate using an *in vivo* ^{13}C-labelling assay.

A. plantensis cells cultivated for 3 d in SOT medium with or without nitrate were transferred to new medium containing $NaH^{13}CO_3$ instead of $NaHCO_3$ to initiate ^{13}C labelling. Intracellular metabolites were extracted and analysed by MS after labelling for 1, 2, 3, 5, 10, 20, and 30 min in order to assess metabolic turnover. The ratio of ^{13}C to total carbon in each metabolite [i.e. the ^{13}C fraction (%)] was calculated from mass isotopomer distributions determined by MS. As ionized compounds are separated by mass in MS and the data are presented as *m*/*z*, the *m*/*z* of a ^{13}C-labelled compound increases by an amount equal to the number of stable isotope atoms incorporated (Shastri and Morgan, 2007; Hasunuma et al., 2010). Therefore, by determining the ratio of the intensity of the monoisotopic ion to that of its isotopic ions, the ratio of stable isotope-labelled to unlabelled metabolite can be determined. As the pool size of some metabolites, such as

sugar phosphates and sugar nucleotides, is small in cyanobacteria, the MRM detection method was optimized for each compound in order to maximize the sensitivity of detection (Supplementary Table S2).

In an *in vivo* ^{13}C-labelling assay, ^{13}C is assimilated through the Calvin cycle enzyme ribulose-1,5-bisphoshate carboxylase/oxygenase (Rubisco) in the form of $^{13}CO_2$ used in the production of 3-phosphoglycerate (3PGA) from ribulose-1,5-bisphoshate (RuBP) (Fig. 4A). In our experiments, the size of the 3PGA pool remained almost constant during ^{13}C labelling, while the ^{13}C fraction associated with 3PGA increased linearly up to 3 min (Fig. 5). These data suggested that ^{13}C assimilation was kept in a steady state. The ^{13}C fraction associated with sugar phosphates involved in the Calvin cycle and glycogen biosynthesis increased with time and reached a plateau at 10 min (Fig. 6). The ^{13}C-labelling ratio did not reach 100% for any metabolite identified.

In the presence of nitrate, the fraction of ^{13}C associated with 3PGA reached a maximum of 80.3% after 30 min of labelling, but in the absence of nitrate reached only 62.5%. Nitrate depletion resulted in a decrease in the ^{13}C-labelling ratio for other sugar phosphates, such as dihydroxyacetone phosphate, F6P, G1P, G6P, phosphoenolpyruvate, ribose-5-phosphate, ribulose-5-phosphate, sedoheptulose-7-phosphate, and xylulose-5-phosphate, as well as sugar nucleotides such as ADP-Glc. Nitrate depletion also resulted in a decrease in the ^{13}C fraction for most amino acids, with the exceptions of glutamate and glutamine, which showed an increase in the ^{13}C fraction (Fig. 6). In summary, nitrate depletion resulted in an increase in the cellular glycogen content, while the turnover of intermediates involved in the biosynthesis of glycogen from CO_2 was not promoted with carbon derived from $^{13}CO_2$. These results indicated that, under conditions of nitrate depletion, glycogen is biosynthesized with carbon derived from photosynthetic products.

Discussion

Cultivation under conditions of nitrate deficiency leads to a significant increase in the glycogen content in *A. platensis* and *Synechocystis* sp. PCC6803 cells. In cyanobacteria, glycogen is normally synthesized from CO_2 assimilated during periods of light exposure (Ball and Morell, 2003). In the present study, dynamic metabolic profiling using a ^{13}C-labelling assay revealed that when nitrate is unavailable, the carbon skeleton of glycogen is synthesized with carbon derived from photosynthetic products other than CO_2. The observed decrease in protein accumulation and the transient increase in amino acid levels concomitant with glycogen production suggest the possibility that glycogen is biosynthesized with carbons derived from amino acids released from proteins via gluconeogenesis. The ^{13}C fractions calculated for glycogen precursors (F6P, G1P, G6P, and ADP-Glc) and amino acids based on our ^{13}C-labelling experiments support this possibility.

Nitrogen limitation is frequently used to increase the production of cyanobacterial glycogen (Yoo et al., 2007). Glycogen metabolism is important for cyanobacteria in photosynthesis; however, little is known about the mechanism of glycogen biosynthesis in these organisms. To the best of our knowledge, this is the first report demonstrating the temporal metabolic profile of cyanobacteria cultivated under conditions of nitrogen deficiency. Using CE/MS, we were able to reproducibly identify 69 and 77 hydrophilic metabolites in *A. platensis* and *Synechocystis* sp. PCC6803, respectively. As shown in Fig. 4, shifting the cyanobacterial cells into nitrogen depletion and cultivating them for 72 h resulted in global metabolic reprogramming that involved reductions in the levels of several free amino acids that are typically abundant in the cell, such as aspartate, glutamate, and glutamine, and increases in the levels of organic acids such as 2-ketoglutarate, malate, and succinate. Time-course profiling of metabolites demonstrated transient increases in the levels of other amino acids, including glycine, histidine, isoleucine, leucine, methionine, phenylalanine, proline, threonine, and tyrosine. Such transient increases might be caused by protein hydrolysis and subsequent assimilation of these amino acids into glycogen via gluconeogenesis. It is not clear if these responses are common in cyanobacteria and other photosynthetic species. However, several recent reports have demonstrated that cultivation under nitrogen-deficient conditions leads to an increase in starch content with a decrease in protein content

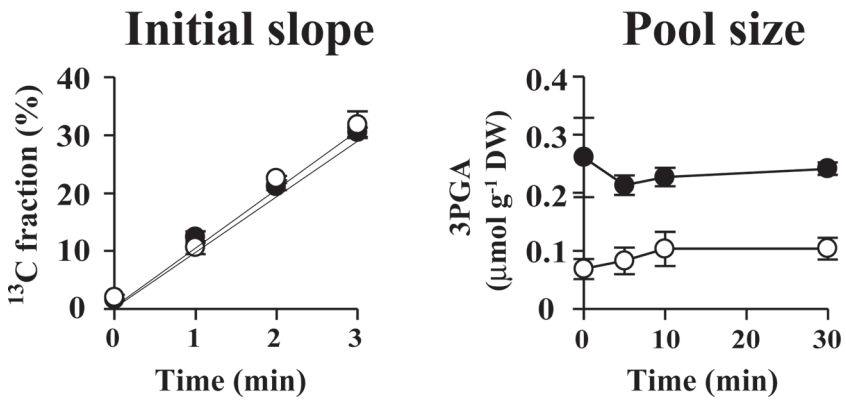

Fig. 5. Initial time course of the ^{13}C fraction and size of the 3PGA pool during ^{13}C labelling of *A. platensis* cells cultivated with (closed circles) or without (open circles) the addition of nitrate. Error bars indicate ±SD (n=3).

in green algae such as *Chlorella vulgaris* and *Dunaliella tertiolecta* (Rismani-Yazdi et al., 2011; Ho et al., 2013). Thus, green algae may show the same metabolic response as *A. platensis* and *Synechocystis* sp. PCC6803 under conditions of nitrogen depletion.

Metabolic profiling using MS enables the determination of a large number of metabolites, including minor intermediates, and provides a snapshot of the metabolic status of a cell at a given point in time. In order to observe fluxes in metabolism, MS analysis combined with *in vivo* labelling

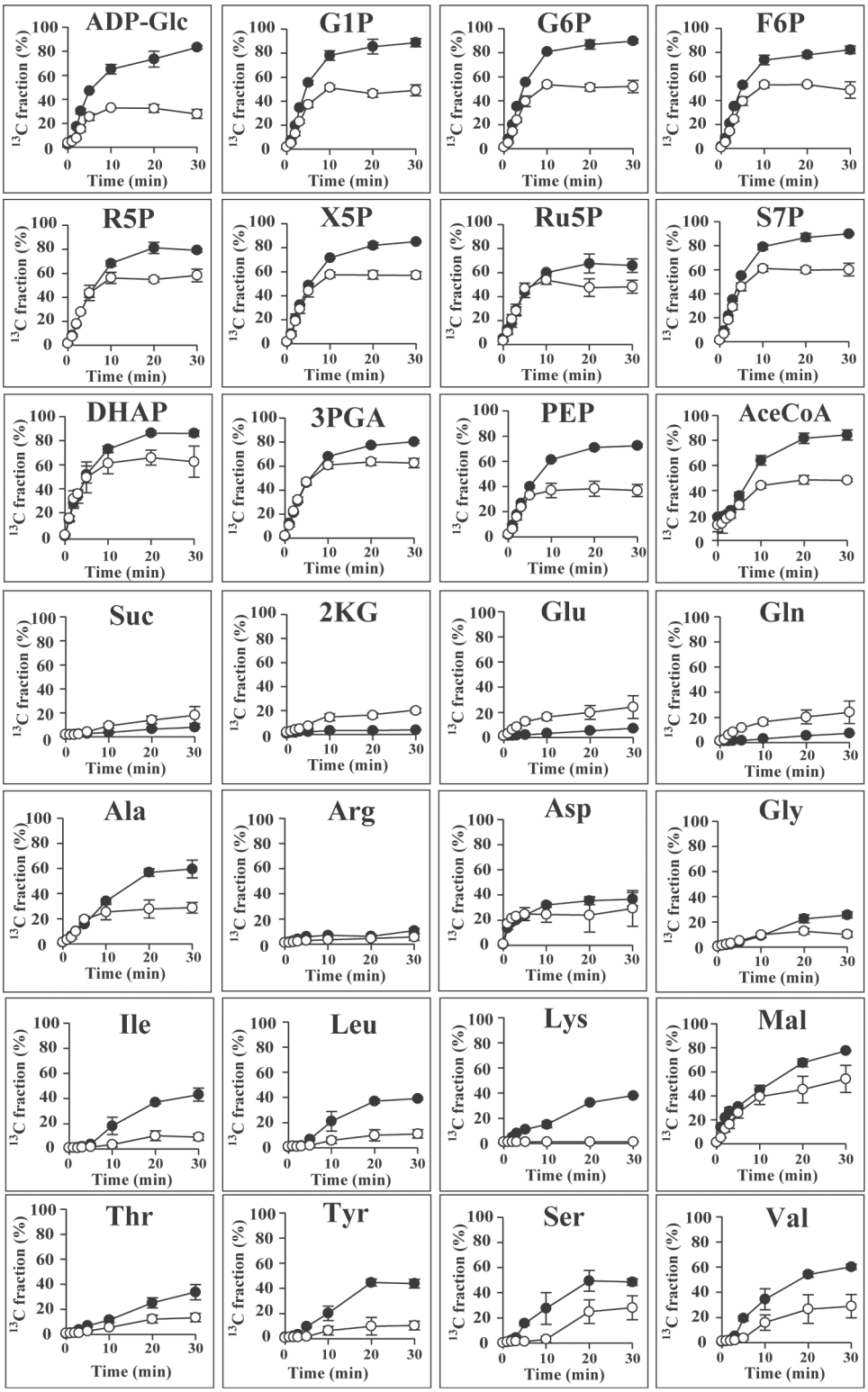

Fig. 6. Time-course analysis of the metabolite ^{13}C fraction of *A. platensis* cells cultivated with (closed circles) or without (open circles) the addition of nitrate. Error bars indicate ±SD (*n*=3).

using a stable isotope is required. Hasunuma et al. (2010) reported that metabolite kinetics can be estimated by measuring changes in the abundance of mass isotopomers over time. In the present study, *in vivo* ^{13}C labelling was performed by replacing the sole carbon source in the cultivation medium with $NaH^{13}CO_3$. Using this technique, we found that the ^{13}C fraction of sugar phosphate compounds increased with time, reaching a plateau within 10 min of labelling initiation. In photosynthetic organisms, Rubisco catalyses the initial reaction in primary carbon fixation involving condensation of CO_2 and RuBP, yielding two molecules of 3PGA. Through the action of the Calvin cycle, 3PGA is converted into triose phosphates, which serve as the initial carbon skeletons for the synthesis of intracellular metabolites (Fig. 4). In our experiments, the turnover rate of sugar phosphates involved in the Calvin cycle was significantly higher than that of organic acids and amino acids. As shown in Fig. 6, the ^{13}C fraction did not reach 100% for any metabolite. Previous studies using leaves of *Nicotiana tabacum* and *Quercus rubra* for ^{13}C labelling also showed less than 90% of the ^{13}C fraction of sugar phosphates (Delwiche and Sharkey, 1993; Hasunuma et al., 2010). Although the reason the ^{13}C fraction tends to peak below 100% remains unknown, one reasonable explanation is that the isotope-labelled carbons compete with carbon atoms derived from internal stores for assimilation into metabolites, ultimately entering an equilibrium phase after the initial linear ^{13}C-enrichment phase.

Remarkably, the maximum value of the ^{13}C fraction was reduced under conditions of nitrate depletion. By limiting the nitrate supply, the ^{13}C fractions of 3PGA, F6P, G6P, G1P, and ADP-Glc declined from 80.3, 82.2, 89.7, 88.7, and 83.2% to 62.5, 48.6, 51.9, 49.1, and 27.7 %, respectively (Fig. 6). The decrease in the maximum ^{13}C fraction points to a reduction in the availability of $^{13}CO_2$ for use in glycogen biosynthesis when the cells are confronted with nitrogen starvation, despite the fact that the glycogen content increases. The ^{13}C fraction of many amino acids also declined following nitrate depletion, indicative of either a reduction in the assimilation of carbon atoms into amino acids or an increase in the generation of free amino acids through protein hydrolysis. Almost no carbon was incorporated into isoleucine, leucine, and lysine under conditions of nitrate depletion, even though the pools of these amino acids increased (Fig. 4). The rate of $^{13}CO_2$ incorporation was not altered by depleting nitrate (Fig. 5). These data support the hypothesis that there is an increase in the release of amino acids from proteins under these conditions. The increase in the ^{13}C fraction of glutamate and glutamine could be due to decreases in the pools of these metabolites.

Depleting the supply of nitrate resulted in a decrease in the protein content in *A. platensis* from 42.7 to 15.4% of the dry cell weight, while the glycogen content increased from 13.7 to 63.2% (Fig. 1). As demonstrated for other cyanobacteria (Grossman et al., 1993), we found that *A. platensis* cells degrade their light-harvesting apparatus, phycobilisome, to provide nitrogen when exogenous nitrogen is limited (Fig. 2). Accordingly, glycogen might be partly synthesized with carbons derived from phycobilisome. Because nitrogen is frequently a limiting nutrient for non-diazotrophic cyanobacteria, these organisms have developed survival strategies that enable them to adapt to nitrogen deprivation. When both *A. platensis* and *Synechocystis* sp. PCC6803 undergo bleaching in response to a lack of nitrogen sources, the cells accumulate excess glycogen as a deposit of intracellular energy. Although the precise role that glycogen plays in cyanobacteria remains unclear, it has been suggested that the accumulation of glycogen by cyanobacteria may be advantageous during starvation periods, providing both a stored source of energy and a carbon surplus (Strange, 1968). Our metabolomic study enhances current understanding of the flow of carbon involved in glycogen biosynthesis during periods of nitrate depletion.

The combination of metabolic profiling and turnover analysis used in the present study, which can be referred as dynamic metabolic profiling, demonstrated that acclimation to nitrogen depletion in cyanobacteria involves coordinated changes in carbon metabolism. To the best of our knowledge, ours is the first report of *in vivo* stable isotope labelling of cyanobacteria cultivated under conditions of nitrate depletion. Direct measurement of metabolic turnover using our *in vivo* ^{13}C-labelling assay provided conclusive evidence that the metabolic profile of cyanobacterial cells cultured in the absence of nitrate changes over time.

Cyanobacteria represent a globally important biomass because they are responsible for a substantial proportion of primary production in the hydrosphere (Partensky et al., 1999). *A. platensis* is a remarkably fast-growing halophilic cyanobacterium capable of accumulating glycogen, and thus has the potential to serve as a feedstock for the fermentative production of biofuels and bio-based chemicals (Aikawa et al., 2012). By controlling light intensity, temperature, and the supplies of nitrate and other nutrients during cultivation, the metabolism and growth of *A. platensis* can be manipulated to further enhance the already exceptional glycogen production capacity of this organism (Aikawa et al., 2012). For utilization of cyanobacteria as biofuel feedstock, maintenance of cell growth is also important to improve glycogen production, because glycogen production should be estimated by multiplying glycogen content per cell by cellular biomass production (Aikawa et al., 2012). Low nitrate supply not only promotes glycogen levels in the cells but also reduces the biomass production. Therefore, in enhancing glycogen production through metabolic engineering, glycogen accumulation should be induced after cell propagation by depleting nitrate. Expression of transgenes involved in metabolic pathway engineering might be controlled by nitrogen-responsive promoters (Imamura et al., 2006).

To date, only a few metabolomic studies of cyanobacteria have been published (Eisenhut et al., 2008; Bennette et al., 2011; Osanai et al., 2011), and ours is the first report of a metabolomic analysis of *A. platensis*. As metabolites are the final downstream products or effects of gene expression, metabolomics is often used to assign or validate functional annotations of genes for enzymes involved in metabolic pathways (Hasunuma et al., 2011; O'Grady et al., 2012). Metabolomic approaches thus provide valuable information for use in designing novel strategies to enhance the productive capacities of microorganisms through genetic engineering.

Synechocystis sp. PCC6803, a unicellular cyanobacterium for which the genome was sequenced in 1996 (Kaneko et al., 1996), is one of the most widely used species in studies of photosynthetic bacteria. Recently, researchers have begun to employ systems biology approaches to obtain a more detailed understanding of metabolic processes in this and other organisms (Weckwerth, 2011; O'Grady et al., 2012). Metabolomics is a particularly important component of systems biology research. Advances in metabolite profiling have opened up the possibility of gaining previously unobtainable insights into physiological adaptation to environmental alterations.

Supplementary data

Supplementary data are available at *JXB* online.

Supplementary Table S1. Analytical validation of CE/MS for the quantification of hydrophilic metabolites in *A. platensis* and *Synechocystis* sp. PCC 6803.

Supplementary Table S2. LC/QqQ-MS parameters used in the analysis of metabolite isotopomers.

Supplementary Table S3. Analytical validation of UPLC/PDA for the quantification of pigments in *A. platensis* and *Synechocystis* sp. PCC6803.

Supplementary Table S4. Temporal changes in metabolite content in *A. platensis* cells after the initiation of cultivation in SOT medium containing 29.4 or 0 mM sodium nitrate.

Supplementary Table S5. Temporal changes in metabolite content in *Synechocystis* cells after the initiation of cultivation in BG11 medium containing 17.6 or 0 mM sodium nitrate.

Supplementary Fig. S1. Temporal changes in metabolite content in *Synechocystis* cells cultivated with or without nitrate.

Acknowledgements

This work was supported by the Precursory Research for Embryonic Science and Technology (PRESTO) program of the Japan Science and Technology Agency.

References

Aikawa S, Izumi Y, Matsuda F, Hasunuma T, Chang JS, Kondo A. 2012. Synergistic enhancement of glycogen production in *Arthrospira platensis* by optimization of light intensity and nitrate supply. *Bioresource Technology* **108,** 211–215.

Akimoto S, Yokono M, Hamada F, Teshigahara A, Aikawa S, Kondo A. 2012. Adaptation of light-harvesting systems of *Arthrospira platensis* to light conditions, probed by time-resolved fluorescence spectroscopy. *Biochimica et Biophysica Acta* **1817,** 1483–1489.

Ball SG, Morell MK. 2003. From bacterial glycogen to starch: understanding the biogenesis of the plant starch granule. *Annual Review of Plant Biology* **54,** 207–233.

Baran R, Reindl W, Northern TR. 2009. Mass spectrometry based metabolomics and enzymatic assays for functional genomics. *Current Opinion in Microbiology* **12,** 547–552.

Bennette NB, Eng JF, Dismukes GC. 2011. An LC-MS-based chemical and analytical method for targeted metabolite quantification in the model cyanobacterium *Synechococcus* sp. PCC 7002. *Analytical Chemistry* **83,** 3808–3816.

Bölling C, Fiehn O. 2005. Metabolite profiling of *Chlamydomonas reinhardtii* under nutrient deprivation. *Plant Physiology* **139,** 1995–2005.

De Marsac NT, Houmard J. 1988. Complementary chromatic adaptation: physiological conditions and action spectra. *Methods in Enzymology* **167,** 318–328.

Delwiche CF, Sharkey TD. 1993. Rapid appearance of ^{13}C in biogenic isoprene when $^{13}CO_2$ is fed to intact leaves. *Plant, Cell and Environment* **16,** 587–591.

Dismukes GC, Carrieri D, Bennette N, Ananyev GM, Posewitz MC. 2008. Aquatic phototrophs: efficient alternatives to land-based crops for biofuels. *Current Opinion in Biotechnology* **19,** 235–240.

Eisenhut M, Huege J, Schwarz D, Bauwe H, Kopka J, Hagemann M. 2008. Metabolome phenotyping of inorganic carbon limitation in cells of the wild type and photorespiratory mutants of the cyanobacterium *Synechocystis* sp. strain PCC 6803. *Plant Physiology* **148,** 2109–2120.

Ernst A, Kirschenlohr H, Diez J, Böger P. 1984. Glycogen content and nitrogenase activity in *Anabaena variabilis*. *Archives of Microbiology* **140,** 120–125.

Flores E, Frías JE, Rubio LM, Herrero A. 2005. Photosynthetic nitrate assimilation in cyanobacteria. *Photosynthetic Research* **83,** 117–133.

Fraser PD, Pinto MES, Holloway DE, Bramley PM. 2000. Application of high-performance liquid chromatography with photodiode array detection to the metabolic profiling of plant isoprenoids. *The Plant Journal* **24,** 551–558.

Garcia DE, Baidoo EE, Benke PI, Pingitore F, Tang YJ, Villa S, Keasling JD. 2008. Separation and mass spectrometry in microbial metabolomics. *Current Opinion in Microbiology* **11,** 233–239.

Grossman AR, Schaefer MR, Chiang GG, Collier JL. 1993. The phycobilisome, a light-harvesting complex responsive to environmental conditions. *Microbiological Reviews* **57,** 725–749.

Hasunuma T, Harada K, Miyazawa S, Kondo A, Fukusaki E, Miyake C. 2010. Metabolic turnover analysis by a combination of *in vivo* ^{13}C-labeling from $^{13}CO_2$ and metabolic profiling with CE-MS/MS reveals rate-limiting steps of the C_3 photosynthetic pathway in *Nicotiana tabacum* leaves. *Journal of Experimental Botany* **61,** 1041–1051.

Hasunuma T, Kondo A. 2012. Development of yeast cell factories for consolidated bioprocessing of lignocellulose to bioethanol through cell surface engineering. *Biotechnology Advances* **30,** 1207–1218.

Hasunuma T, Miyazawa S, Yoshimura S, Shinzaki Y, Tomizawa K, Shindo K, Choi SK, Misawa N, Miyake C. 2008. Biosynthesis of astaxanthin in tobacco leaves by transplastomic engineering. *The Plant Journal* **55,** 857–868.

Hasunuma T, Sanda T, Yamada R, Yoshimura K, Ishii J, Kondo A. 2011. Metabolic pathway engineering based on metabolomics confers acetic and formic acid tolerance to a recombinant xylose-fermenting strain of *Saccharomyces cerevisiae*. *Microbial Cell Factories* **10,** 2.

Ho SH, Huang SW, Chen CY, Hasunuma T, Kondo A, Chang JS. 2013. Bioethanol production using carbohydrate-rich microalgae biomass as feedstock. *Bioresource Technology* **135,** 191–198.

Huege J, Krall L, Steinhauser MC, Giavalisco P, Rippka R, Tandeau de Marsac N, Steinhauser D. 2011. Sample amount alternatives for data adjustment in comparative cyanobacterial metabolomics. *Analytical and Bioanalytical Chemistry* **399,** 3503–3517.

Imamura S, Tanaka K, Shirai M, Asayama M. 2006. Growth phase-dependent activation of nitrogen-related genes by a control network of group 1 and group 2 σ factors in a cyanobacterium. *Journal of Biological Chemistry* **281,** 2668–2675.

John RP, Anisha GS, Nampoothiri KM, Pandey A. 2011. Micro and macroalgal biomass: A renewable source for bioethanol. *Bioresource Technology* **102,** 186–193.

Kaneko T, Sato S, Kotani H, Tanaka A, *et al.* 1996. Sequence analysis of the genome of the unicellular cyanobacterium *Synechocystis* sp. strain PCC6803. II. Sequence determination of the entire genome and assignment of potential protein-coding region. *DNA Research* **3,** 109–136.

Kato H, Izumi Y, Hasunuma T, Matsuda F, Kondo A. 2012. Widely targeted metabolic profiling analysis of yeast central metabolites. *Journal of Bioscience and Bioengineering* **113,** 665–673.

Krall L, Huege J, Catchpole G, Steinhauser D, Willmitzer L. 2009. Assessment of sampling strategies for gas chromatography-mass spectrometry (GC-MS) based metabolomics of cyanobacteria. *Journal of Chromatography B* **877,** 2952–2960.

Mussatto SI, Dragone G, Guimarães PM, Silva JP, Carneiro LM, Roberto IC, Vicente A, Domingues L, Teixeira JA. 2010. Technological trends, global market, and challenges of bio-ethanol production. *Biotechnology Advances* **28,** 817–830.

O'Grady J, Schwender J, Shachar-Hill Y, Morgan JA. 2012. Metabolic cartography: experimental quantification of metabolic fluxes from isotopic labelling studies. *Journal of Experimental Botany* **63,** 2293–2308.

Osanai T, Oikawa A, Azuma M, Tanaka K, Saito K, Hirai MY, Ikeuchi M. 2011. Genetic engineering of group 2σ factor SigE widely activates expressions of sugar catabolic genes in *Synechocystis* species PCC6803. *Journal of Biological Chemistry* **286,** 30962–30971.

Page-Sharp M, Behm CA, Smith GC. 1998. Cyanophycin and glycogen synthesis in a cyanobacterial *Scytonema* species in response to salt stess. *FEMS Microbiology Letters* **160,** 11–15.

Partensky F, Hess WR, Vaulot D. 1999. *Prochlorococcus*, a marine photosynthetic prokaryote of global significance. *Microbiology and Molecular Biology Reviews* **63,** 106–127.

Quintana N, van der Kooy F, van de Rhee MD, Voshol GP, Verpoorte R. 2011. Renewable energy from cyanobacteria: energy production optimization by metabolic pathway engineering. *Applied Microbiology and Biotechnology* **91,** 471–490.

Rippka R, Deruelles J, Waterbury JB, Herdman M, Stanier RY. 1979. Generic assignments, strains histories and properties of pure culture of cyanobacteria. *Journal of General Microbiology* **111,** 1–61.

Rismani-Yazdi H, Haznedaroglu BZ, Bibby K, Peccia J. 2011. Transcriptome sequencing and annotation of the microalgae *Dunaliella tertiolecta*: pathway description and gene discovery for production of next-generation biofuels. *BMC Genomics* **12,** 148.

Rittmann BE. 2008. Opportunities for renewable bioenergy using microorganisms. *Biotechnology and Bioengineering* **100,** 203–212.

Santillan C. 1982. Mass production of *Spirulina*. *Experientia* **38,** 40–43.

Sarcina M, Mullineaux CW. 2004. Mobility of the IsiA chlorophyll-binding protein in cyanobacterial thylakoid membrane. *Journal of Biological Chemistry* **279,** 36514–36518.

Shastri AA, Morgan JA. 2007. A transient isotopic labeling methodology for ^{13}C metabolic flux analysis of photoautotrophic microorganisms. *Phytochemistry* **68,** 2301–2312

Soga T, Heiger DN. 2000. Amino acid analysis by capillary electrophoresis electrospray ionization mass spectrometry. *Analytical Chemistry* **72,** 1236–1241.

Strange RE. 1968. Bacterial "glycogen" and survival. *Nature* **220,** 606–607.

Weckwerth W. 2011. Green systems biology – from single genomes, proteomes and metabolomes to ecosystems research and biotechnology. *Journal of Proteomics* **75,** 284–305.

Yoo SH, Kappel C, Spalding M, Jane JL. 2007. Effects of growth condition on the structure of glycogen produced in cyanobacterium *Synechocystis* sp. PCC6803. *International Journal of Biological Macromolecules* **40,** 498–504.

Yoshida S, Imoto J, Minato T, *et al.* 2008. Development of bottom-fermenting *Saccharomyces* strains that produce high SO_2 levels, using integrated metabolome and transcriptome analysis. *Applied and Environmental Microbiology* **74,** 2787–2796.